Material-Independent 3D Patterning Via Two-Photon Lithography and Discontinuous Wetting

Zheqin Dong, Joël Monti, Haijun Cui, Alexander Welle, Surya A. Singaraju, Eva Blasco,* and Pavel. A. Levkin*

The fabrication of complex 3D structures composed of micrometer-sized features made of different functional materials is an immensely important and yet highly challenging task. Here, a method is developed to fabricate multi-material 3D structures with micrometer precision by combining macroscopic 3D printing (digital light processing), with two-photon lithography (2PL) and material-independent discontinuous dewetting. Specifically, 3D inherently superhydrophobic objects are first printed by DLP, followed by creating hydrophilic micropatterns on their surface using 2PL. By exploiting the effect of discontinuous wetting, the selective deposition of solutions of functional materials into microscopic hydrophilic regions on the surface of 3D structures, with high resolution and great design flexibility is demonstrated. Importantly, the method is material-independent and enables the micropatterning of a variety of functional materials dispersed in aqueous solutions including polydopamine, silica, or Ag nanoparticles. As an exemplary application, it is shown that conductive Ag electrodes can be created on the curved surface of 3D-printed objects to construct structural electronics. The flexibility, high resolution, and material diversity in designing multimaterial 3D structures open exciting new functionalities and possibilities in a variety of applications including advanced electronics, soft robotics, and chemical or bioengineering.

1. Introduction

Fabrication of complex 3D structures composed of micrometer-sized features made of different functional materials is an immensely important goal that still remains largely unsolved. Until now, traditional photolithography is the most advanced manufacturing technology for creating micro/nanostructures incorporating different materials, enabling the fabrication of architectures with distinct material properties (conducting, insulating, and semiconducting).[1] Photolithography, however, heavily relies on costly photomasks and is usually limited to simple geometries and to a few specialized materials (such as silicon, copper, silicon dioxide, and silicon nitride). Two-photon lithography (2PL) (also known as 3D laser printing and previously known as direct laser writing (DLW)), is an emerging light-triggered 3D printing technology based on two-photon polymerization, which allows fabrication of 3D structures with high geometrical complexity at the microscale. The multimaterial printing using this technology is still in its infancy.[2] While a few studies reported the manufacturing of multimaterial 3D microstructures by sequential printing of different inks,[3–9] these methods are quite complex and time consuming, and the usage of materials such as microparticles, nanoparticles, or non-(photo)polymerizable species requires further development.

To date, only a few studies have explored 2PL to micropattern 3D structures by photografting using acrylate polymerization,[10] Diels–Alder cycloaddition[11,12] or addition-fragmentation chain transfer.[13] In spite of their ability to create 3D chemical patterns

Z. Dong, H. Cui, P. A. Levkin
Institute of Biological and Chemical Systems – Functional Molecular Systems (IBCS-FMS)
Karlsruhe Institute of Technology (KIT)
Hermann-von-Helmholtz-Platz 1, 76344 Eggenstein-Leopoldshafen, Germany
E-mail: levkin@kit.edu

The ORCID identification number(s) for the author(s) of this article can be found under https://doi.org/10.1002/admt.202201268.

J. Monti, S. A. Singaraju, E. Blasco
Institute of Nanotechnology
Karlsruhe Institute of Technology (KIT)
Hermann-von-Helmholtz-Platz 1, 76344 Eggenstein-Leopoldshafen, Germany
A. Welle
Institute of Functional Interfaces (IFG) and
Karlsruhe Nano Micro Facility (KNMF)
Karlsruhe Institute of Technology (KIT)
Hermann-von-Helmholtz-Platz 1, 76344 Eggenstein-Leopoldshafen, Germany
E. Blasco
Institute of Organic Chemistry
Heidelberg University
69120 Heidelberg, Germany
E-mail: eva.blasco@oci.uni-heidelberg.de
E. Blasco
Centre for Advanced Materials
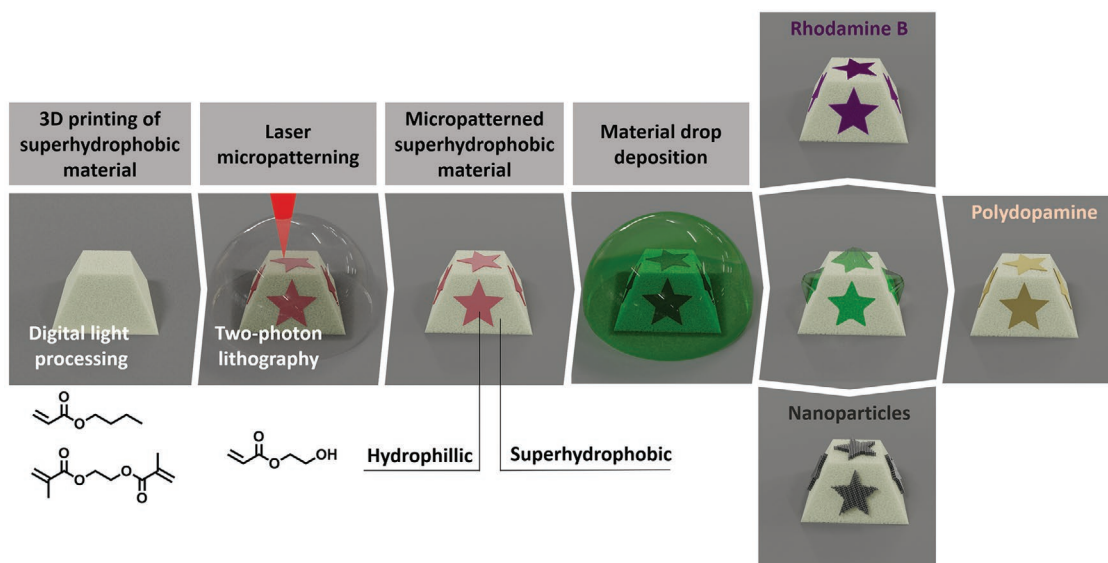Heidelberg University
69120 Heidelberg, Germany

**ADVANCED
SCIENCE NEWS**

www.advancedsciencenews.com

**ADVANCED
MATERIALS
TECHNOLOGIES**

www.advmattechnol.de

Figure 1. A schematic showing the method for creating multimaterials 3D micropatterned objects detailed in this work. a) Fabrication of a macroscopic superhydrophobic 3D polymer structure by DLP. Ink composition: 30 wt% butyl acrylate, 20 wt% ethylene glycol dimethacrylate, 50 wt% 1-decanol. b) Creation of hydrophilic micropatterns on the top and side surfaces of the DLP-printed objects by 2PL. Ink composition: hydroxyethyl acrylate. c,d) Exposure to and confinement of an aqueous solution of functional materials onto the hydrophilic micropatterns using the effect of discontinuous wetting. e) Formation of micropatterns of functional materials deposited in hydrophilic regions upon solvent evaporation.

with very fine resolution, these methods can only change the surface properties of patterned regions at the surface chemistry level. To realize the further patterning of functional materials, the deposited materials with very strong chemical affinity to the grafted molecules is required,[10] which greatly limits the scope of deposited functional materials.

Discontinuous dewetting is a powerful method to pattern and deposit functional materials on surfaces. In discontinuous dewetting, patterns with extreme wettability difference (e.g., hydrophilicity and superhydrophobicity) lead to the spontaneous break of a bigger droplet and formation of smaller droplets, confined to the hydrophilic regions of predefined geometries and driven by the dewetting of liquid on the superhydrophobic background.[14–16] Due to its simplicity, scalability, and versatility, this strategy has been used for applications including optical waveguides,[17] flexible electronics,[18] and miniaturized biological screenings.[19] Although discontinuous dewetting has been applied to 2D surfaces, its potential to pattern 3D objects remains to be explored. A recent study used a mask covering technique to create hydrophilic-superhydrophobic patterns on 3D aluminum structures.[20] However, this method is limited to macroscale patterning (resolution of several millimeters) and simple geometries (stripes and circles).

In this study, we introduce a new method for creating multimaterial 3D structures. The approach combines macroscopic 3D printing, specifically digital light processing (DLP), with micrometer precise 2PL and material-independent discontinuous dewetting, allowing 3D micropatterning/assembly of functional materials with enormous design flexibility (**Figure 1**). We use DLP combined with polymerization-induced phase separation[21,22] to print inherently superhydrophobic 3D objects (Figure 1a), followed by creating hydrophilic, water adhesive, micropatterns on the surface of the superhydrophobic 3D objects using 2PL (Figure 1b). The effect of discontinuous

dewetting allows us to selectively and precisely deposit solutions of functional materials onto the hydrophilic regions of the surface of the 3D structures (Figure 1c–e). Thanks to the design flexibility of 2PL, this strategy allows for the site-specific patterning of materials, both on the top and side areas of 3D macroscopic objects with micrometer resolution. We demonstrate that a variety of functional materials, including small molecule dyes, silica nanoparticles, and conductive Ag nanoparticles, can be deposited on the 3D objects with high spatial control. In addition, we show the possibility of surface chemical functionalization happening inside microdroplets deposited via discontinuous dewetting, using polydopamine deposition as an example. Thus, our method opens a new path toward fabrication of multimaterial 3D structures with locally encoded properties, which is crucial for achieving future complex and multifunctional devices and architectures.

2. Results and Discussion

To 3D print superhydrophobic objects via DLP, we have developed an ink consisting of a hydrophobic monomer (butyl acrylate), a crosslinker (ethylene glycol dimethacrylate), a porogen (1-decanol), and a photoinitiator Irgacure 819.[22] The porogenic solvent leads to in situ phase separation during DLP printing, affording an inherently porous nanostructured material (**Figure 2**a). Such porous structures can not only render the surface of the 3D-printed object superhydrophobic, but also amplify the hydrophilicity of the hydrophilic patterns created by 2PL. This extreme contrast of wettability is critical to ensure the effect of discontinuous wetting and site-specific material patterning. As shown in Video S1 (Supporting Information), the DLP-printed truncated pyramid demonstrated excellent water repellency with very low water adhesion (with a pull-off force of about 3 µN as measured by scanning
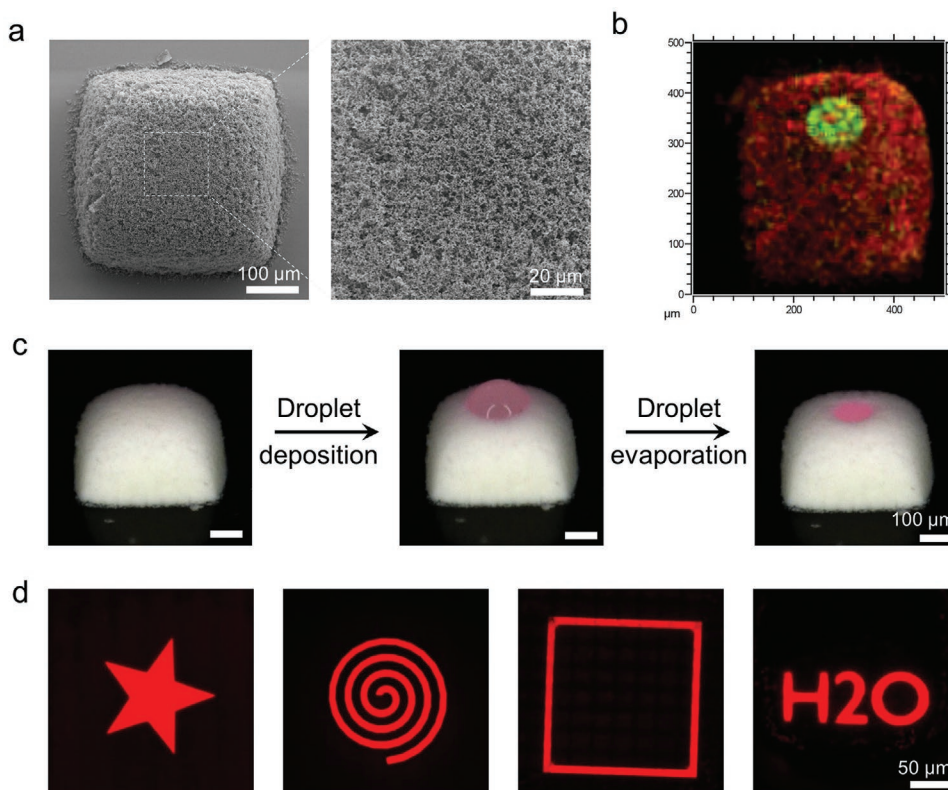
**ADVANCED
SCIENCE NEWS**

www.advancedsciencenews.com

**ADVANCED
MATERIALS
TECHNOLOGIES**

www.advmattechnol.de

Figure 2. Demonstration of the overall process using a fluorescent dye (RhB) as an exemplary material. a) SEM images and b) ToF-SIMS maps of the 2PL micropatterned truncated pyramid. Green: Sum of $C_2H_3O^-$, C_2OH^-, and $C_3H_3O_2^-$; red: Sum of C_2H^-, $C_3H_5^-$, C_4H^-, and $C_2H_3O^-$. 128×128 pixel, 5-point averaging in the image. c) Snapshots of a video (Video S3, Supporting Information) showing the deposition and evaporation of a dyed water droplet (RhB) on the hydrophilic-superhydrophobic patterned truncated pyramid. d) Confocal fluorescence microscope images showing various fluorescence patterns formed on the hydrophilic-superhydrophobic patterned truncated pyramid via discontinuous wetting.

droplet adhesion microscopy[22]). In a second step, hydrophilic patterns were created on the superhydrophobic objects by acrylate polymerization-mediated photografting, using 2PL. The micropatterning was performed by exposing the superhydrophobic structures to a hydrophilic monomer, 2-hydroxyethyl acrylate (HEA), in the presence of a photoinitiator, Irgacure 819 (2 wt%). Due to the incomplete conversion during DLP printing process, considerable amounts of methacrylate groups remain unreacted on the surface of the printed structures as proved by the ATR-FTIR spectroscopy (Figure S1, Supporting Information). Upon laser exposure, these unreacted (meth)acrylate groups can react with the growing chains of polyHEA to achieve covalent surface grafting, which changes the surface wettability and generates hydrophilic micropatterns. It is also possible that polyHEA physically adsorbs to the surface. To evaluate this, the DLP-printed porous structures were immersed into a polyHEA solution, followed by washing and drying steps (see the Experimental Section for details). However, since the produced surface remained superhydrophobic (Video S2, Supporting Information), we can conclude that the produced hydrophilic patterns are due to the covalent surface grafting of polyHEA and not because of its physical adsorption. The optimization of the patterning parameters (noticeably laser power and scanning speed) were carried out based on the evolution of the patterning quality and reliability with respect to the variation of these parameters. It was observed that scanning speed above 10 000 μm s^{-1} resulted in decreasing patterning quality and reliability. Laser

power lower than 35 mW resulted in unreliable, incomplete or unsuccessful patterning, while laser power up to 50 mW lead to an increasingly significant deterioration of the surface morphology (Figure S2, Supporting Information). The optimized parameters (10 000 μm s^{-1} scanning speed, 35 mW laser power) were chosen to the optimize time-efficiency of the process, the retention of the morphology of the surfaces through the patterning process, determined by SEM imaging (Figure 2a), as well as to optimize the definition and reliability of the micropatterning.

The photografting of HEA onto the hydrophobic structure by 2PL was evidenced by time-of-flight secondary ion mass spectrometry (ToF-SIMS). Due to several molecular similarities in the building blocks of the main polymer used for DLP and the poly(2-hydroxyethyl acrylate) used for functionalization, only a small number of fragments in the SIMS data showed the material contrast on the produced patterns at this stage: $C_2H_3O^-$, C_2OH^-, $C_3H_3O_2^-$, and phosphates. The former three fragments can be cleaved from the side chain in poly(2-hydroxyethyl acrylate) and are represented in green in Figure 2b, whereas the substrate polymer is imaged in red based on the observed fragments C_2H^-, $C_3H_5^-$, C_4H^-, and $C_2H_3O^-$. Phosphate signals are attributed to the used photoinitiator. Reference spectra obtained from unreacted Iragcure 819 showed a very strong PO_2^- signal (original data are provided in the repository Radar4KIT). Furthermore, in unreacted Irgacure TOF-SIMS analysis finds the molecular signal for $C_{26}H_{27}PO_3^-$ and $C_{26}H_{26}PO_3^-$ with matching

isotope patterns. This signal is not found in case of reacted photoinitiator since the initiator is degraded and incorporated into a long polymer chain, leaving behind the PO_2^- signal.

To demonstrate the working principle of our strategy and the formation of hydrophilic patterns on a superhydrophobic surface, we first used a water droplet containing a fluorescent dye, rhodamine B (RhB). When the aqueous droplet contacted the patterned pyramid, only the micrometric region (200 µm diameter circle) functionalized with the hydrophilic poly(2-hydroxyethyl acrylate) was wetted, and a "daughter" droplet remained adhered with a shape conformal to the pattern geometry (Figure 2c; and Video S3, Supporting Information). Such a discontinuous wetting effect results from the combination of the superhydrophobicity of the 3D object, and the high hydrophilicity of the patterned circular region due to the presence of polar groups created by 2PL. The surface is probably superhydrophilic but since it is hard to measure the contact angles on the micrometer sized spots, we will refer to these regions as hydrophilic. Upon droplet evaporation, the RhB from the aqueous solution, remained deposited on the hydrophilic regions and could be readily visualized (Figure 2c). It is worth noticing that the surface structure of the patterned region experienced an obvious shrinkage due to the capillary forces generated during water evaporation (Figure S3, Supporting Information). Thanks to the high-resolution and versatility of 2PL, complex micropatterns (including a star, a spiral, a ring and letters) with very high definition could be created on top of the DLP-printed truncated pyramid and functionalized with RhB, the visualization of these patterns by confocal fluorescence microscopy in shown by Figure 2d.

The selective surface functionalization of 3D objects with micrometer precision promises unique applications in various fields including microelectronics, robotics, optics, microreactors, and bioengineering. Although techniques for microscale surface functionalization on 2D surfaces have been well-established, only a few are applicable to 3D structures, including electron-beam lithography (EBL),[23] 2PL,[2] and dip-pen nanolithography (DPN).[24] These techniques, however, are developed for a particular type of material (e.g., EBL demands electron-sensitive resist, 2PL needs photoreactive functional species, DPN usually requires molecular inks), and therefore require significant developments for each new material or component.[2,23,24] In contrast, as our method combines 2PL and discontinuous wetting for site-specific material deposition, it is almost material-independent as long as the material can be dissolved or dispersed in an aqueous solution. Other materials that can be formed in situ via a reaction inside the droplet can also be used. Therefore, our approach opens new possibilities to micropattern 3D objects with various materials and achieve previously inaccessible properties and functionalities. As a proof-of-principle test for the functionalization of surfaces nonparallel to the substrate, we first created hydrophilic patterns both on the top and side areas of a 3D-printed pyramid. The patterned structure was immersed in an aqueous RhB solution and then immediately taken out and visualized under a microscope. **Figure 3** shows the dye patterns left on the top and side surfaces of 3D structures after droplet evaporation, indicating that only the 2PL patterned regions were wetted by the solution, leading to the selective dye deposition.

We next demonstrate the material-independence of our method by selective deposition of several functional materials, including dopamine for polydopamine-based surface functionalization, as well as silica and silver nanoparticles. Polydopamine is a substrate-independent surface coating material widely used to construct functional surfaces with versatile properties such as biocompatibility, antifouling, conductivity, or catalytic activity.[25–27] We created polydopamine micropatterns on the DLP-printed objects by simply immersing them into a dopamine Tris-buffer (pH 8.5) solution for 1 h. The formation of polydopamine patterns is visualized by optical microscopy and further confirmed by ToF-SIMS characterization (**Figure 4**a). Some discrete flakes were also found on the truncated pyramid. This might be attributed to the highly adhesive property of polydopamine, which adsorbs to the polymer globules of superhydrophobic substrates, leading to partial wetting during the submerging process.[28,29] This can be potentially improved by using perfluorinated (instead of aliphatic) superhydrophobic substrates to reduce adsorption and prolong the lifetime of superhydrophobicity. Importantly, the selective deposition of polydopamine serves as an example to demonstrate the ability of our method to not only pattern materials soluble/dispersible in water, but also materials that can be in situ formed via reactions happening inside microdroplets. Such ability opens an additional possibility to pattern materials that are difficult to dissolve/disperse, for example, conductive polymers or polymer gels.

The precise patterning of micro/nanoparticles is important for both fundamental research and practical applications such as sensing, catalysis, advanced optics, or organic electronics.[30–33] However, the selective deposition of particles at the microscale is challenging, especially on 3D surfaces.[19] Here, we show that our patterning based on discontinuous dewetting can be applied not only to small molecule solutions, but also to nanoparticles dispersions. Figure 4b shows 2.5D patterns of silica nanoparticles formed via discontinuous dewetting on a truncated pyramid. Interestingly, the silica nanoparticles self-organize into well-ordered arrays during the droplet evaporation.

Creating conductive patterns on 3D objects is central to the fabrication of advanced structural electronics, and has previously been realized by direct printing of conductive inks.[34] However, the resolution of most extrusion/jetting based printing techniques is still quite limited.[35–37] Our method, on the other hand, allows for the patterning of conductive materials on 3D-printed objects at the micrometer scale. Thanks to the thermal stability of the DLP-printed structures, Ag nanoparticles were successfully patterned and further annealed (150 °C, 30 min) on the surface of 3D-printed pyramids, as proved by both optical and SEM-EDX microscopy (Figure 4c; and Figure S4. Supporting Information). Electrical measurements showed a conductivity of the Ag patterned regions (line width 50 µm, length 300 µm) with a corresponding resistance of about 350 Ω, while the 3D porous substrate (without patterning) was an insulating material ($R > G\Omega$) (Figure 4d). These results demonstrate the ability of this method to fabricate structural microelectronic devices combining the functionality of electronic circuits with 3D design flexibility, which are useful in advanced antennas, sensors or transistors.
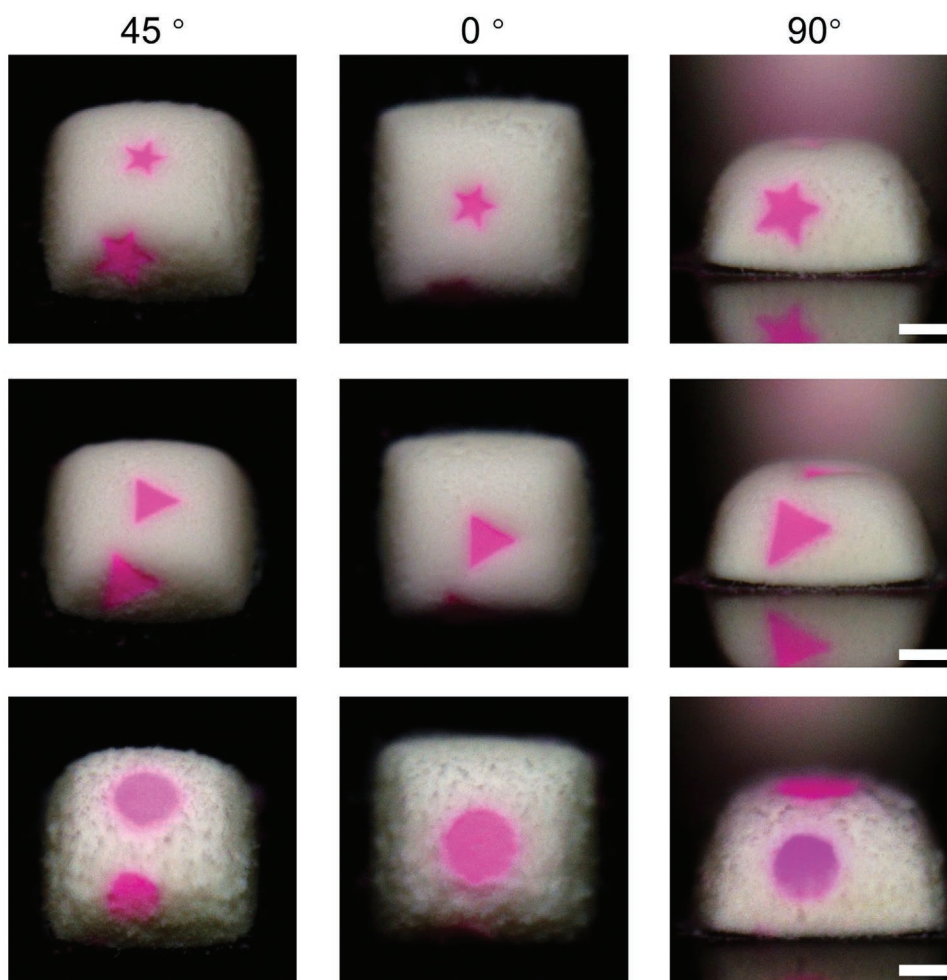
Figure 3. Demonstration of the possibility to micropattern material solutions on the side surface of 3D objects. Digital microscope images (taken at different angles) showing the dye patterns formed on the top and side areas of the 3D structures, indicating that only the 2PL micropatterned regions were wetted by the material solution due to the effect of discontinuous wetting. Scale bars 100 µm.

3. Conclusion

In this work, we proposed a methodology enabling material-independent micropatterning of 3D surfaces by combining 2PL and discontinuous wetting. This method allows for precise micropatterning of various functional materials (including dyes, polydopamine, nanoparticles) both on the upper surface and side areas of 3D objects, with very high spatial resolution and geometrical freedom. As a proof-of-concept application, we fabricate conductive Ag microelectrodes on 3D surface. It is foreseeable that our approach is applicable to many more functional materials that are water dispersible or can be in situ formed via reaction inside the aqueous droplet including, inter alia, proteins, quantum dots, conductive polymers, and polymer gels. We believe that the micrometer precision, design flexibility, ability to pattern 3D surfaces and material-independence of this strategy will pave the way to a new generation of multimaterial 3D structures with unprecedented properties and functionalities, opening exciting opportunities in numerous applications from advanced microelectronics, and sensors to microreactors and bioengineering.

4. Experimental Section

Materials and Chemicals: Irgacure 819 (Ig819) was purchased from VWR and all the other chemicals were purchased from Sigma-Aldrich and used without further purification.

DLP 3D Printing of Superhydrophobic Objects: The inks used for DLP 3D printing consisted of 30 wt% butyl acrylate as the monomer, 20 wt% ethylene glycol dimethacrylate (EDMA) as the crosslinker, 50 wt% 1-decaol as the porogenic solvent, and 2 wt% Ig819 as the photoinitiator. All components were mixed in an amber vial and ultrasonicated in a sonic bath (Elmasonic S 30H, frequency 37 kHz and power 80 W) for 30 min to obtain a homogenous ink solution.

The superhydrophobic 3D structures were printed by using a commercial desktop DLP printer (Miicraft Prime 110). The printer is based on a LED projector (385 nm) with an intensity of 1.0 mW cm^{-2} at the vat and a XY resolution of 40 µm. After printing, the 3D-printed objects were immersed in acetone for 24 h to remove the unreacted monomers and porogens.

2PL Patterning of 3D-Printed Structures: The superhydrophobic truncated pyramids were taken out of acetone and rapidly immersed in the patterning mixture, hydroxyethyl acrylate (98 wt%) and Ig819 (2 wt%). 2PL was performed using a Photonic Professional GT instrument (Nanoscribe GmbH), using a laser with a central wavelength of 780 nm, with a 25×/NA 0.8 objective lens (Zeiss LCI Plan-Neofluar 25×/0.8) in

**ADVANCED
SCIENCE NEWS**

www.advancedsciencenews.com

**ADVANCED
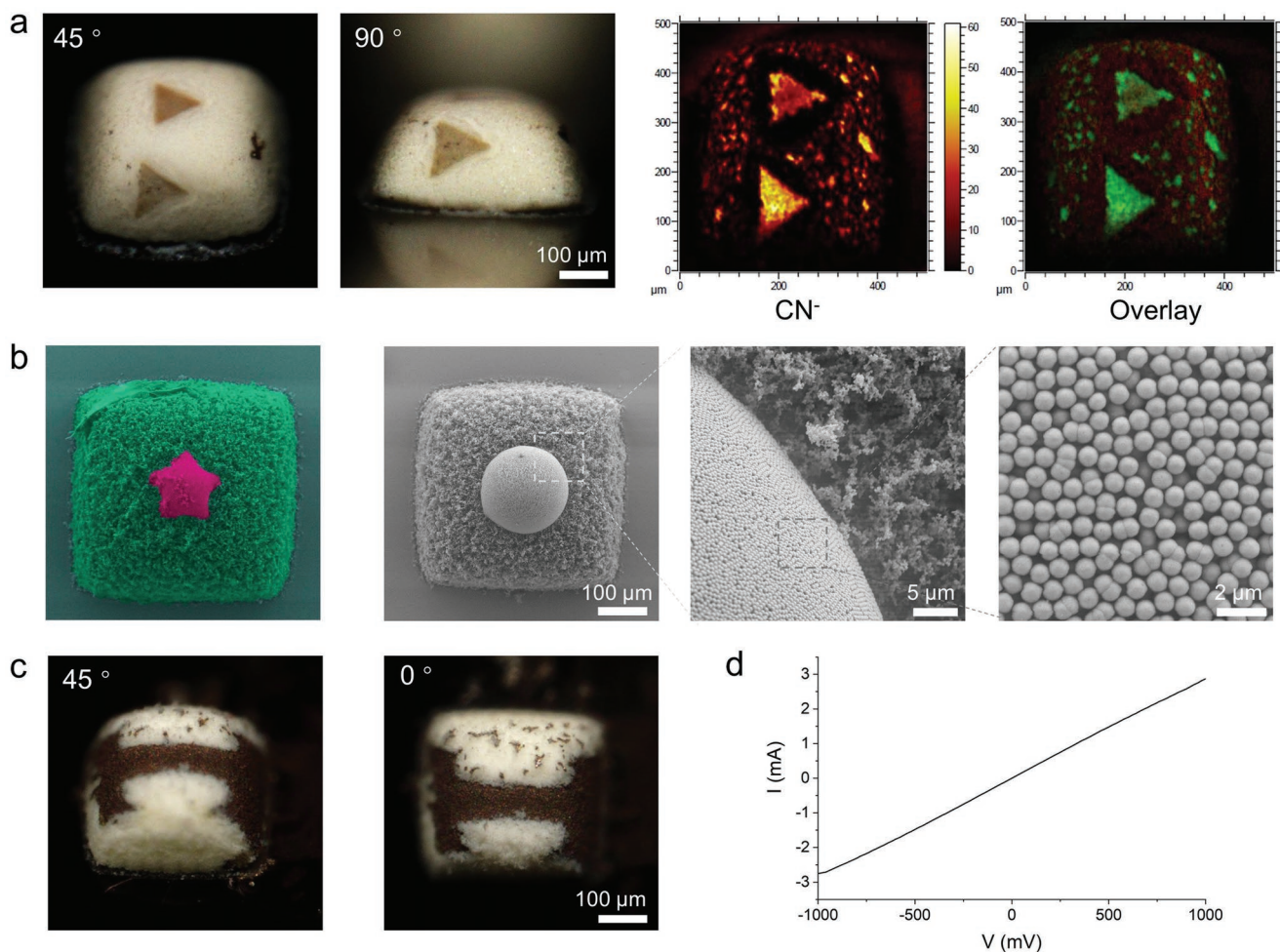MATERIALS
TECHNOLOGIES**

www.advmattechnol.de

Figure 4. Selective deposition of a variety of functional materials on the surface of 3D objects. a) Digital microscope images and ToF-SIMS mapping of the polydopamine patterns on the 3D objects. In the ToF-SIMS overlay, the sum of O^- together with $C_2H_3O^-$, indicating the truncated pyramid substrate polymer is shown in red, and the sum of CN^- and both Cl isotopes, highlighting the polydopamine in green. b) SEM images of 2.5D micropatterns of silica nanoparticles ($d = 900$ nm) formed on the 3D objects. The left image is false colored: the superhydrophobic truncated pyramid is colored in green, and the deposited silica nanoparticles are colored in red. c) Digital microscope images (top and 45° angle view) of a conductive Ag patterns formed via discontinuous dewetting on an insulating truncated pyramid. d) A representative I–V curve measured from the Ag patterned region (line width 50 μm, length 300 μm).

dip-in mode. The focal point was manually set at photoresist–glass substrate interface prior to any lateral stage translation. The volumes for patterning were scanned using galvanometer scanners in the xy-plane and objective translation along the z-axis, with a scanning speed of 10 000 μm^{-s} and a laser power of 35 mW. The scanned volumes were constructed with a hatching distance of 0.5 μm and a slicing distance of 1 μm. If relevant, the volumes were split using $250 \times 250 \times 100$ μm^3 rectangular domains. The scanned volumes were constructed with the xy-origin along their center-of-mass and aligned on the truncated pyramid manually. A semiautomatic alignment of the scanned volumes on the truncated pyramids, using a preliminary manual coordinate spotting, was used for the conductive patterns. The scanned volumes for the surfaces parallel to the glass substrate were constructed as 100 μm tall right prisms of the patterns, located at 60 and 40 μm below and above the theoretical z-location of the surface. The scanned volumes for angled surfaces were constructed as 50 μm tall right prism of the patterns, and angled according to the theoretical angle of the surfaces.

All the printing jobs were computed using DeScribe, and from STL files constructed using Blender.

Supercritical Drying: The 2PL patterned objects were first immersed in acetone for 24 h for solvent exchange, followed by CO$_2$ supercritical

drying to avoid shrinkage of the nanoporous structures, which is crucial to render the object superhydrophobic.[22] Briefly, the patterned objects immersed in acetone were first transferred to the chamber of the supercritical apparatus (Leica EM CPD030). Then, acetone was replaced by liquid CO$_2$ by repeatedly flushing with liquid CO$_2$ and releasing the acetone. Subsequently, the chamber temperature and pressure were increased to 35 °C and 90 bar to maintain the CO$_2$ in supercritical condition. Finally, the chamber pressure was gradually dropped to atmospheric pressure to release the CO$_2$. The entire supercritical drying process took about 40 min.

Physical Adsorption Test of polyHEA on the DLP-Printed Porous Structures: To clarify whether the polyHEA patterns on the surface are either due to covalent binding or physical adsorption of polyHEA, the DLP-printed porous structures were immersed into a 10 wt% polyHEA (M_n 3.2×10^4 g mol^{-1}, M_w 1.4×10^5 g mol^{-1}, measured by DMAc-GPC) ethanolic solution for 24 h. Then the structures were subjected to the same acetone exchange and CO$_2$ supercritical drying as denoted above. The dried 3D structures remain their superhydrophobicity as shown in Video S2 (Supporting Information), indicating that the physical adsorption of polyHEA to the porous surfaces is either insignificant in 2PL or is washed away during the drying process.

**ADVANCED
SCIENCE NEWS**

www.advancedsciencenews.com

**ADVANCED
MATERIALS
TECHNOLOGIES**

www.advmattechnol.de

Material Deposition: Deposition of Rhodamine B, silica nanoparticles and silver nanoparticles. The aqueous material solutions were first prepared as follows: 0.5 mg mL^{-1} RhB solution was obtained by dissolving RhB in water, 1 wt% silica nanoparticle suspension was prepared by diluting a commercial silica dispersion (5 wt%, $d = 900$ nm, Sigma) with water, and 2 wt% silver nanoparticle suspension was prepared by diluting a commercial silver ink (30 wt% in ethylene glycol, Sigma) with water. Then, a droplet (3 μL) of the material solution was used to cover the 2PL-patterned 3D structures, and subsequently retracted by a pipette. Due to the effect of discontinuous wetting, a daughter droplet was left on the 2PL hydrophilic micropatterns, while the unmodified regions remained un-wetted. Upon the evaporation of the daughter droplet, the materials in the solution remained deposited in the hydrophilic micropatterns (Figure 1). For Ag nanoparticle patterned objects, a further annealing step was performed at 150 °C for 30 min.

Deposition of polydopamine. The 2PL-patterned 3D structures were immersed in a 2 mg mL^{-1} 3-hydroxytyramine hydrochloride tris-buffer solution (tris solution: 10 mм, pH 8.5, Sigma) for 1 h and taken out.

Digital Microscopy: Digital microscope images of the samples were obtained by a Keyence BZ 9000. The images were taken at several different angles to reveal the 3D structure.

Confocal Microscopy: Confocal microscope images of the samples patterned with fluorescent dyes (Rhodamine B) were taken by Zeiss LSM 800. Due the highly porous nature of the 3D-printed objects, they were not transparent enough for making 3D z-stack images, therefore only dye patterns on the top surfaces of the 3D structure were visualized.

Scanning Electron Microscopy (SEM) and Energy-Dispersive X-Ray (EDX) Mapping: The samples were sputter-coated with a 10 nm gold layer, and imaged using a Zeiss Leo 1530 scanning electron microscope operating at 5.0 kV.

Time-of-Flight Secondary Ion Mass Spectrometry (ToF-SIMS): ToF-SIMS was performed on a TOF.SIMS5 instrument (ION-TOF GmbH, Münster, Germany). This spectrometer is equipped with a Bi cluster primary ion source and a reflectron type time-of-flight analyzer. UHV base pressure was $<2 \times 10^{-9}$ mbar. For good mass and lateral resolution the Bi source was operated in "delayed extraction" mode providing unbunched Bi$_3^+$ primary ion pulses at 25 keV energy. Delayed extraction mode further reduces topography artefacts and charging effects. Despite that an electron flood gun was used to compensate sample charging. The primary ion beam was rastered across a 500×500 μm^2 field of view on the sample, and 128×128 or 256×256 data points were recorded. Spectra were calibrated on the omnipresent OH$^-$, C$_2^-$, C$_2$H$^-$, C$_3^-$, and C$_3$H$^-$ peaks. Based on these datasets the chemical assignments for characteristic fragments were determined. Raw data and analysis files are available on Radar4KIT (https://doi.org/10.35097/570).

Conductivity Test: The electrode patterns were contacted by source measurement unit (SMU) needles prolonged with a thin gold wire. *I–V* curves from −1 to 1 V were recorded using an Agilent 4156C parameter analyzer. The resistance is extracted from the slope of the *I–V* curves and is computed on Origin.

Supporting Information

Supporting Information is available from the Wiley Online Library or from the author.

Acknowledgements

Conflict of Interest

The authors declare no conflict of interest.

Data Availability Statement

The data that support the findings of this study are available from the corresponding author upon reasonable request.

Keywords

[1] J. Richard, *Introduction to Microelectronic Fabrication*, Prentice Hall, Upper Saddle River, NJ **2002**.

[2] Y. Liang, M. Frederik, H. F. B. Uwe, B. Eva, W. Martin, *Light Adv. Manuf.* **2021**, *2*, 296.

[3] F. Mayer, S. Richter, J. Westhauser, E. Blasco, C. Barner-Kowollik, M. Wegener, *Sci. Adv.* **2019**, *5*, eaau9160.

[4] A. C. Lamont, M. A. Restaino, M. J. Kim, R. D. Sochol, *Lab Chip* **2019**, *19*, 2340.

[5] M. Gernhardt, H. Frisch, A. Welle, R. Jones, M. Wegener, E. Blasco, C. Barner-Kowollik, *J. Mater. Chem. C* **2020**, *8*, 10993.

[6] S. K. Saha, T. M. Uphaus, J. A. Cuadra, C. Divin, I. S. Ladner, K. G. Enstrom, R. M. Panas, *Precis. Eng.* **2018**, *54*, 131.

[7] Z.-C. Ma, Y.-L. Zhang, B. Han, X.-Y. Hu, C.-H. Li, Q.-D. Chen, H.-B. Sun, *Nat. Commun.* **2020**, *11*, 4536.

[8] P. Kunwar, Z. Xiong, Y. Zhu, H. Li, A. Filip, P. Soman, *Adv. Opt. Mater.* **2019**, *7*, 1900656.

[9] R. A. Farrer, C. N. LaFratta, L. Li, J. Praino, M. J. Naughton, B. E. A. Saleh, M. C. Teich, J. T. Fourkas, *J. Am. Chem. Soc.* **2006**, *128*, 1796.

[10] H. Ceylan, I. C. Yasa, M. Sitti, *Adv. Mater.* **2017**, *29*, 1605072.

[11] B. Richter, T. Pauloehrl, J. Kaschke, D. Fichtner, J. Fischer, A. M. Greiner, D. Wedlich, M. Wegener, G. Delaittre, C. Barner-Kowollik, M. Bastmeyer, *Adv. Mater.* **2013**, *25*, 6117.

[12] T. K. Claus, B. Richter, V. Hahn, A. Welle, S. Kayser, M. Wegener, M. Bastmeyer, G. Delaittre, C. Barner-Kowollik, *Angew. Chem. Int. Ed.* **2016**, *55*, 3817.

[13] X. Wu, B. Gross, B. Leuschel, K. Mougin, S. Dominici, S. Gree, M. Belqat, V. Tkachenko, B. Cabannes-Boué, A. Chemtob, A. Spangenberg, *Adv. Funct. Mater.* **2022**, *32*, 2109446.

[14] R. J. Jackman, D. C. Duffy, E. Ostuni, N. D. Willmore, G. M. Whitesides, *Anal. Chem.* **1998**, *70*, 2280.

[15] M. D. Neto, A. Stoppa, M. A. Neto, F. J. Oliveira, M. C. Gomes, A. R. Boccaccini, P. A. Levkin, M. B. Oliveira, J. F. Mano, *Adv. Mater.* **2021**, *33*, 2007695.

[16] Y. Yang, L.-P. Xu, X. Zhang, S. Wang, *J. Mater. Chem. B* **2020**, *8*, 8101.

[17] A. Kumar, M. Whitesides George, *Science* **1994**, *263*, 60.

[18] Z. Wang, H. Cui, S. Li, X. Feng, J. Aghassi-Hagmann, S. Azizian, P. A. Levkin, *ACS Appl. Mater. Interfaces* **2021**, *13*, 21661.

[19] W. Feng, E. Ueda, P. A. Levkin, *Adv. Mater.* **2018**, *30*, 1706111.

[20] J.-W. Lee, K. Kim, G. Ryoo, J. Kim, J. Vinoth Kumar, W. Hwang, *Appl. Surf. Sci.* **2022**, *576*, 151849.

[21] Z. Dong, H. Cui, H. Zhang, F. Wang, X. Zhan, F. Mayer, B. Nestler, M. Wegener, P. A. Levkin, *Nat. Commun.* **2021**, *12*, 247.

[22] Z. Dong, M. Vuckovac, W. Cui, Q. Zhou, R. H. A. Ras, P. A. Levkin, *Adv. Mater.* **2021**, *33*, 2106068.

[23] Y. Chen, *Microelectron. Eng.* **2015**, *135*, 57.

[24] G. Liu, S. H. Petrosko, Z. Zheng, C. A. Mirkin, *Chem. Rev.* **2020**, *120*, 6009.

[25] H. Lee, M. Dellatore Shara, M. Miller William, B. Messersmith Phillip, *Science* **2007**, *318*, 426.

[26] J. H. Ryu, P. B. Messersmith, H. Lee, *ACS Appl. Mater. Interfaces* **2018**, *10*, 7523.

[27] T. G. Barclay, H. M. Hegab, S. R. Clarke, M. Ginic-Markovic, *Adv. Mater. Interfaces* **2017**, *4*, 1601192.

[28] S. M. Kang, I. You, W. K. Cho, H. K. Shon, T. G. Lee, I. S. Choi, J. M. Karp, H. Lee, *Angew. Chem., Int. Ed.* **2010**, *49*, 9401.

[29] L. O. Prieto-López, P. Herbeck-Engel, L. Yang, Q. Wu, J. Li, J. Cui, *Adv. Mater. Interfaces* **2020**, *7*, 2000876.

[30] A. N. Shipway, E. Katz, I. Willner, *ChemPhysChem* **2000**, *1*, 18.

[31] J. Huang, F. Kim, A. R. Tao, S. Connor, P. Yang, *Nat. Mater.* **2005**, *4*, 896.

[32] X. Ye, L. Qi, *Nano Today* **2011**, *6*, 608.

[33] H.-N. Barad, H. Kwon, M. Alarcón-Correa, P. Fischer, *ACS Nano* **2021**, *15*, 5861.

[34] D. Espalin, D. W. Muse, E. MacDonald, R. B. Wicker, *Int. J. Adv. Manuf. Technol* **2014**, *72*, 963.

[35] A. Joe Lopes, E. MacDonald, R. B. Wicker, *Rapid Prototyping J.* **2012**, *18*, 129.

[36] F. Tricot, C. Venet, D. Beneventi, D. Curtil, D. Chaussy, T. P. Vuong, J. E. Broquin, N. Reverdy-Bruas, *RSC Adv.* **2018**, *8*, 26036.

[37] X. Peng, X. Kuang, D. J. Roach, Y. Wang, C. M. Hamel, C. Lu, H. J. Qi, *Addit. Manuf.* **2021**, *40*, 101911.